Tellus (1981), *33*, 242–253

Prediction of stratiform clouds: Results from a 5-day forecast with a global model

By HILDING SUNDQVIST, *Department of Meteorology, University of Stockholm, Arrhenius Laboratory, S-106 91 Stockholm, Sweden*[1]

(Manuscript received December 1, 1980; in final form January 30, 1981)

ABSTRACT

A parameterization scheme of stratiform condensation including cloud water content as a prognostic variable (Sundqvist, *Q. J. Roy. Met. Soc.*, 1978) is implemented in a global numerical prediction model. A phenomenological investigation of the model cloud behaviour during a 5-day integration is carried out. In the analysis the resulting clouds have been grouped into three classes, low, middle and high, so that a colour picture presentation is possible. Those pictures are also compared with satellite pictures. Furthermore, some details of the model cloud water content and cover are shown with the aid of cross-sections. The results exhibit a good deal of realism and it is suggested that further experiments be performed in which dynamical effects for the model clouds are analyzed.

1. Introduction

In an earlier paper, Sundqvist (1978), henceforth called SQJ, the present author proposed a parameterization scheme of stratiform condensation and clouds to be used in numerical weather prediction models and GCMs. There are two particular features of that approach, namely, cloud water content is an explicit prognostic variable and the cloud cover is allowed to be partial (sub-grid scale). In SQJ a few numerical applications were carried out with a one-dimensional model (vertical coordinate) by which a rough idea is obtained of the model characteristics with regard to the micro-physical parameterization and the response to a given forcing.

Further quantitative experiments involving this model of stratiform condensation have recently been undertaken, now within a model for medium range prediction. The purpose of the present paper is to demonstrate the performance of the condensation model when incorporated in its proper complex. The present investigation is limited to a study of the appearance of stratiform clouds during the model integration. The radiation scheme of the prediction model was switched off in the experiment implying that dynamic interaction between condensation and the rest of the flow field occurs only via release of latent heat. An investigation of the dynamical effects on the model atmosphere from these clouds is hence saved for a later occasion.

In the present experiments, the global grid-point prediction model of the European Centre for Medium Range Weather Forecasts (ECMWF) has been used. Numerical values of constants and parameters are given in SI units.

2. The prediction model and the parameterization scheme for stratiform condensation

Only those features of the ECMWF prediction model that are relevant in the present context will be given here. For a more complete description of that model, reference is made to JSC (1980) or Burridge and Haseler (1977) and Tiedtke et al. (1979). We shall dwell somewhat longer on a recapitulation of the parameterization scheme proposed in SQJ.

[1] Contribution no. 431.

0040-2826/81/030242-12$02.50/0

2.1. *Some features of the prediction model*

In addition to the advective terms (adiabatic part), the ECMWF prediction model has the following processes incorporated: horizontal and vertical eddy diffusion, radiation (which is switched off in the present experiment) and moist convection; the large scale condensation is replaced by the parameterization scheme of stratiform condensation that is discussed in SQJ.

The horizontal diffusion is described by a fourth order operator applied to momentum, temperature and water vapour mixing ratio. The term is mainly regarded as a smoothing function for suppressing computational noise (JSC, 1980).

In the elaborate treatment of vertical eddy diffusion, the calculation of surface fluxes is based on similarity theory and the fluxes above the surface layer are obtained from a K-theory approach applied at all levels of the model atmosphere. Effects of wind shear and static stability are taken into account in all those formulations. The temperature at the earth's surface is pre-assigned over sea for each forecast period; over land areas the surface temperature is obtained from an energy budget equation.

The parameterization of moist convection follows the scheme of Kuo. The vertical coordinate is sigma (= pressure normalized by surface pressure).

The model atmosphere has 15 levels; the three first ones above the ground are situated at σ = 0.996, 0.967 and 0.914. Above those, the separation between the sigma-levels is about 0.07 to 0.09. The mesh-size in the latitude–longitude grid is 1.875° × 1.875° (N48). An enstrophy-conserving, centred differences scheme with a semi-implicit time-stepping is employed. The method of non-linear normal mode initialization is used.

2.2. *The model for stratiform condensation and clouds*

We will not go into the discussions which serve as a basis for the model suggested in SQJ, but merely state its formulation.

Since cloud water content is a dependent variable of the model, there is a need for parameterization of the micro-physical processes governing the growth of cloud droplets into precipitating drops. Furthermore, as sub-grid scale appearance of stratiform condensation will be taken into account, this aspect also requires a parametric relation. It should be mentioned that the sub-grid scale parameterization here refers to the horizontal meshes. In the vertical direction, the condensation is hence assumed to fill the grid-box from its bottom to its top.

In order to give the details of the condensation model, we write those equations of the whole model system that are directly involved, that is, the thermodynamic equation, the prognostic equations for water vapour and for cloud water, and the parametric relations.

$$\frac{\partial T}{\partial t} = A_T + \frac{L}{c_p} Q \tag{2.1}$$

$$\frac{\partial q}{\partial t} = A_q - Q \tag{2.2}$$

$$\frac{\partial m}{\partial t} = -\mathbb{V} \cdot \nabla m - \dot{\sigma} \frac{\partial m}{\partial \sigma} - \frac{\partial}{\partial \sigma} (\dot{\Sigma} m) + Q - P + (1 - b)E \tag{2.3}$$

$$Q = (A_q - U \frac{c_p}{L} S_q A_T + U q_s \frac{1}{p^*} \frac{\partial p^*}{\partial t} - q_s \frac{\partial U}{\partial t} \times (1 + U S_q)^{-1} = M - q_s \frac{\partial U}{\partial t} (1 + U S_q)^{-1} \tag{2.4}$$

$$\frac{\partial U}{\partial t} = \frac{U_s - U}{q_s (U_s - U_0) + m} (M_0 + E) \tag{2.5}$$

$$P = c_0 [1 e^{-(m/m_r]^2}] \, m = c_m m \tag{2.6}$$

$$E(\sigma) = k_E [U_s - \hat{U}] \, [\tilde{P}(\sigma)]^{1/2};$$

$$\hat{U} = \begin{cases} U_0 \text{ if } m > 0 \\ U \text{ if } m = 0 \end{cases} \tag{2.7}$$

$$\dot{\Sigma} = k_\Sigma m^{2/3}; \quad k_\Sigma \sim 1.5 \times 10^{-3} \tag{2.8}$$

$$b = \frac{U - U_0}{U_s - U_0}; \quad \begin{cases} 0 < b \leqslant 1 \text{ if condensation} \\ b \equiv 0 \quad \text{otherwise} \end{cases} \tag{2.9}$$

The notations are as follows (the model parameters will be introduced in the next paragraph):

T	virtual temperature
q	specific humidity
m	water mixing ratio of stratiform clouds

A_T, A_q	all terms except those connected with stratiform condensation
$\mathbb{V}, \nabla$	horizontal wind vector and operator respectively
$\dot{\sigma}$	vertical wind component in the sigma-system
Q (s^{-1})	net heating resulting from stratiform net condensation/evaporation; expressed in equivalents of water mixing ratio
$U = q/q_s$	relative humidity
P (s^{-1})	rate of release of precipitation
$\tilde{P}$ (kg m^{-2} s^{-1})	rate of precipitation
E (s^{-1})	rate of evaporation from rain
$\dot{\Sigma}$	average terminal fall velocity of cloud water in the sigma-system
b	partial cloud cover
p^*	surface pressure

$$S_q = \frac{\varepsilon L^2}{Rc_p} \cdot \frac{q_s}{T^2}; \quad \varepsilon = 0.622$$

$M_0 = M(U = U_0)$

L	latent heat of condensation
R	gas constant for dry air
c_p	specific heat of air at constant pressure

subscript s denotes saturation value, e.g., $U_s \equiv 1$.

The following quantities are the parameters of the model for stratiform condensation:

- c_0 typical time-scale for the rate of conversion of cloud droplets into raindrops in an efficiently precipitating cloud
- m_r characteristic value of cloud water mixing ratio around which a cloud reaches a fully precipitating stage
- k_E time-scale parameter for evaporation from rain
- k_Σ time-scale parameter for terminal fall velocity of cloud water
- U_0 threshold value of relative humidity (< 1) at which condensation may appear

The combined effect of c_0 and m_r, that is c_m in (2.6), is a typical response-time of cloudiness to changes in the synoptic situation (primarily in Q).

The relation describing evaporation from raindrops (2.7) is derived from the rate equation for condensation/evaporation of a single drop (Mason, 1971). To obtain an average rate, a mean fall speed ($\simeq 5$ m s^{-1}) of rain is assumed and the Marshall–Palmer (1948) drop-size distribution is adopted for integration to precipitating mass per unit volume. This is a more well-defined derivation and formulation than the one employed in SQJ.

The average terminal velocity of cloud water (which was not considered in SQJ) is obtained by assuming a log-normal droplet-size distribution in the cloud and the terminal speed of individual droplets to be given by Stoke's law. Then an approximate transformation to the σ-system is done via the hydrostatic relation, neglecting surface pressure tendency. The numerical value of k_Σ indicated in (2.8) is based on an assumed droplet number concentration of about 10^8 m^{-3}; other parameter values of the log-normal distribution are taken from Matveev (1967).

In addition to U_0, the sub-grid scale parameterization is made up by relation (2.5), the deduction of which is given in SQJ. Here, it is sufficient to state that (2.5) is based on the assumption that the relative humidity in the clear parts of a partially cloudy grid-box remains at the threshold value U_0. The definition of partial cloud cover (2.9) is consistent with derivations and assumptions of the model.

2.3. *Brief description of the handling of the condensation terms in the prediction model*

It is the present author's opinion that our understanding of how to treat condensation in dynamical models is not good enough to allow a handling of a mixture of convective and stratiform condensation in a grid-box. Consequently, possible condensation calculations at each time-step and grid-point are here carried out according *either* to a scheme for parameterization of convection, *or* to a scheme for stratiform condensation.

If the advection of m yields a positive m-tendency at any grid-point where $m = 0$ at the previous time-step, an immediate evaporation is assumed of the cloud water advected into the grid-box.

Evaporation from rain is only allowed to take place in the cloud-free portions, $(1 - b)$, of a grid-box. At all grid-points without stratiform condensation the evaporation from rain and from cloud elements as described above, is the only contribution to the stratiform Q. If stratiform condensation is taking place, then proper account for evaporation from rain is taken via relation (2.5).

This evaporation also requires a modification of the precipitation intensity according to (2.7). In the present experiments a linear relation between the evaporation and the precipitation has been employed (without real motivation) as well as a first order accuracy calculation of the modified precipitation rate. The value of k_E was then chosen so that the rate of evaporation yields the same as the one of (2.10) for a precipitation rate of 1 mm h^{-1}.

Note that condensation calculations are carried out even for $Q < 0$ if $m > 0$; this situation implies cloud-dissipation.

The space and time filters adopted in the prediction model (see JSC, 1980) are also applied to the cloud water content, implying that numerically small, negative values of m may arise at some grid-points. A similar effect is likely to be caused on the upstream side of cloudy regions by the centred differing scheme. So, at the end of each time-step, a check on the new m values is performed and negative values are brought to zero.

A detailed description of the handling of the condensation terms is found in Sundqvist (1980).

3. Experiments and results

The results, regarding the evolution of stratiform clouds, of one 5-day prediction on real data will be presented here. In addition to this reference experiment a few more have been performed in which some of the parameters of the cloud model have been varied. Those additional runs have not been complete in various senses and therefore a direct comparison with the reference experiment cannot be done. Where comparisons have been possible, it is clearly indicated that the resulting differences in cloud evolution are small, with the parameter variations employed. The overall features of the results to be presented here, are hence representative. It should be noted, however, that those seemingly small differences in the clouds themselves are in some cases systematic. Therefore, subsequent dynamical differences (mainly via radiation) may cause more distinct differences in the evolving circulations of the model atmosphere. As mentioned earlier these aspects are left for a separate investigation.

The set of parameter values employed in the reference experiment is the following:

$c_0 = 10^{-4}\,s^{-1}$
$m_r = 0.5 \times 10^{-3}$
$U_0 = 0.8$
$k_E = 10^{-3}$ SI units (as described in Subsection 2.3)
$k_\Sigma = 0$

The initial time of the prediction is 00 GMT 16 January 1979. The initial data consist of the conventional meteorological fields, that is, there is no field of cloud water content available. Hence, this has to be put to zero initially.

3.1. *Some integral features of the condensation in the model*

To get a general ideal of the condensation occurring in the prediction model, we first plot some global integrals that are related to condensation. Fig. 1 shows the total cloud water (expressed in kg m^{-2}) in the model atmosphere as a function of time. The figure also contains curves for the rate of precipitation from stratiform condensation and from convection and the net flux of water vapour from the earth's surface; all three quantities are computed as 3-hour means in terms of mm/day. The figure exhibits a feature that appears in most model integrations, namely that it takes a considerable time—in this case about 24–30 hours—to reach a quasi-steady state in the integrated precipitation intensity. This is mainly due to lacking

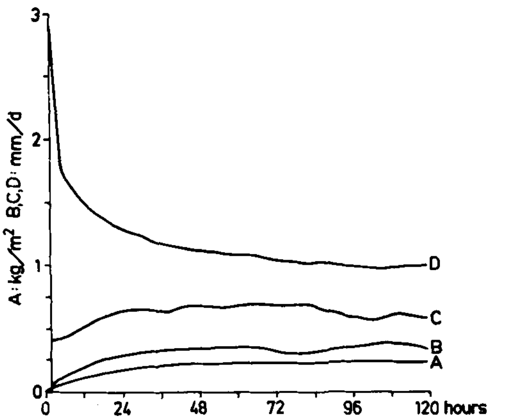

Fig. 1. Time variations of predicted global averages of stratiform cloud water content in kg m^{-2}, curve A; 3-hour mean rates of precipitation, stratiform curve B, convective curve C and of evaporation at the earth's surface, curve D.

initialization of the humidity fields. The time required to reach quasi-equilibrium in the present experiment is longer than normally observed because of the initial absence of stratiform clouds. Not until those have been built up does the precipitation become substantial.

The absolute values in Fig. 1 of the vapour flux and the precipitation intensities are far too small; the climatological flux—and hence also the sum of stratiform and convective precipitation—is about two and a half times larger. The reasons for this discrepancy have not been investigated. A possible reason might be the leaving out of radiation processes or not well tuned parameters (e.g., the threshold value U_0). Reports on investigations at ECMWF with the complete model do show that those figures then are close to the climatological ones (see e.g., Hollingsworth et al., 1980).

The global average of cloud water content is about 0.23 kg m^{-2} (except for the initial build-up period) as shown by curve A in Fig. 1. To the author's knowledge there is no climatological figure, based on measurements, with which to compare. Pruppacher and Klett (1979) estimate a figure of 0.5 kg m^{-2} by making assumptions about global coverage, mean depth and average water content. So their figure probably has an uncertainty of at least 20–30%. Furthermore, it should be noted that the figure obtained in the experiment is related to stratiform clouds alone, while the estimated value is supposed to include also convective clouds. In the present situation—that is, with lacking representative measurements of cloud quantities—we thus have to find the most reasonable value of cloud water content by parameter varying in a series of model integrations in which radiational processes are accounted for.

3.2. *Bird's-eye view of the model clouds*

In this subsection we will make a global observation of the model clouds and their evolution. It is of course not meaningful to map a time-series of all fifteen levels of the model; such a display would just provide an indigestible amount of information. So we group the clouds into the three categories, low, middle and high by vertical summation of the cloud water mixing ratio over the layers $1 \geqslant \sigma \geqslant 0.72$, $0.72 \geqslant \sigma \geqslant 0.37$ and $0.37 \geqslant \sigma$ respectively. This simplified summation is adopted since the objective here is to give more of a qualitative than a quantitative depiction. Having only three vertical classes of clouds it is possible to make a composite, informative picture by utilizing colours.

Before turning to displays of clouds, some characteristic data of model water content will be given. In places where clouds appear the following values may be regarded as typical mean mixing ratios: $0{\cdot}30 \times 10^{-3}$, $0{\cdot}35 \times 10^{-3}$ and 0.15×10^{-3}, or in terms of concentration, 0.27 g m^{-3}, 0.25 g m^{-3} and 0.05 g m^{-3} for low, middle and high clouds respectively. In the densest parts (small regions connected with fronts), the above values are 50–75% larger.

For completeness, it deserves mentioning that the analyses of model data are based on values from every fourth grid-point (every second in each direction) as well as linear interpolations. Hence certain features might look smoother than they have been in the computations.

Low clouds are reproduced in red, middle clouds in yellow and high clouds in blue. The dyeing in the individual classes is made heavier with increasing mixing ratio. In places with deep cloud layers, mixed colours appear. If the vertical sum of cloud water mixing ratio in each category is less than a certain value at a point this is considered to be cloudfree; those sums are 0.18×10^{-3}, 0.15×10^{-3} and 0.05×10^{-3} for the low, middle and high clouds respectively. These lower limits correspond to an average mixing ratio of about 0.05×10^{-3}, 0.04×10^{-3} and 0.01×10^{-3} in the three classes; or as concentrations, 0.04 g m^{-3}, 0.03 g m^{-3} and 0.003 g m^{-3}. These numbers show that only very thin clouds are left out.

The division of the model clouds into three classes enables us to make comparisons with satellite pictures taken in the infrared (IR) wavelengths. In these photographs the clouds are reproduced in grey shading from dark grey for warm (low) cloud tops to white for the coldest (highest) cloud tops. It should be remembered that the model pictures contain exclusively stratiform clouds, whilst the satellite pictures in addition contain convective clouds. The latter pictures hence appear more cloudy especially in lower latitudes where moderately deep cumuli are common (e.g., in the trade wind regions).

Layer clouds are, to a great extent, connected with middle and high latitude frontal systems, so we first exhibit the computed clouds on polar stereographic projection. Plate 1 contains the northern hemisphere clouds at prediction times day 1 through day 5. The predicted 85 kPa geopotential field at the corresponding time is superposed in order to show the positions of the clouds relative to the motion field of the model atmosphere; note that on day 4, the 85 kPa temperature is superposed. The satellite photographs from TIROS-N of the last 2 days of the period are also displayed on Plate 1. A direct comparison between these pictures and those of the prediction is not possible because the former are mosaics, implying that they cover a 24-hour period around the disc as indicated by the GMT clock at the circumference of the pictures. To facilitate the comparison, the predicted clouds at days 3.5 and 4.5 are also shown. Note that the prediction as a whole yields an evolution that simulates reality very well. This is of course a prerequisite for details of the circulation, such as areas of condensation, to develop realistically.

We clearly notice a build-up time, which is a result of having no clouds at initial time of the integration. Not until after 2 days does the cloud amount appear as quasi-steady. This feature is more pronounced for the high clouds than for the middle and low clouds. A probable explanation is that the initial humidity field is more smooth and underestimated at high altitudes than at low ones.

The displays of Plate 1 show that the computed stratiform clouds appear where the 85 kPa circulation indicates existence of frontal and baroclinic zones. The very deep cloud layers (mixed colours), pointing out places of pronounced precipitation, are seen as relatively narrow bands immediately ahead of or in the troughs of the low pressure areas. The day 4 picture shows that the clouds have a realistic position relative to the temperature field; the deep frontal clouds occur in the zones of warm air advection.

The more widespread cloud covers consist, by and large, of either low clouds or high clouds, in both cases with a low water content. The former ones may be regarded as stratocumulus decks, which typically appear in the rear of the frontal waves where presumably a temperature inversion in the lowest levels prevents convection. A detailed example of this feature will be given in the next subsection.

The series of cloud maps on Plate 1 makes it possible to observe that the cloud model describes formation as well as dissipation of clouds with a good deal of realism. Watching, for example, the temporal cloud situation at a fixed geographical point, it is found that a whole spectrum of cloudiness, from clear (or near cloudless) skies to overcast with deep nimbostratus, could be witnessed. Furthermore, it is seen that the predicted clouds of individual frontal systems are well verified by the satellite photographs.

It is interesting to notice that the low and middle clouds exist almost exclusively poleward of approximately latitude 35°, while the high clouds appear in low latitudes as well. So, the model seems to handle realistically not only the cirrus clouds connected with the baroclinic or jet-stream zones but also cirri in the tropical regions where those clouds often are extensions of the tops (anvils) of cumulonimbi in areas of deep convection. If this inference is valid, we note a discrepancy between forecast and observation over the equatorial central Pacific (roughly 160° E–160° W and 0°–10° N). There is a vast area of cold (cirrus) clouds, probably emanating from intense, deep convection, showing up on all three satellite images, while this is missing on the forecast pictures. This comparison of observed and predicted clouds thus provides a hint of a possible failure of the prediction model to bring about convection in an area of large dimensions and with long duration.

The model cirrus clouds are possibly unrealistically abundant over areas of high pressure. However, the water mixing ratio is low (there amounting to $0{\cdot}1 \times 10^{-3}$ for the vertical sum) and the cover (not shown) is about 30%. This observation should be investigated further. The fairly pronounced cloudiness in the high pressure over central Europe resembles what is often observed in winter-time highs in this region.

Pictures taken from geostationary satellites are also useful for comparisons since an instantaneous view of the whole disc (as seen from the satellite) is obtained. To enable a comparison between predicted and observed cloud evolutions over the whole prediction period, the calculated clouds have been transferred to the same projection as the GOES-WEST photographs (IR images) have (Plate 2). This satellite is centred over the equator at longitude 135° W. The predicted 50 kPa isohypses at respective time are superposed on the forecast cloud pictures.

Plate 2 again shows that the stratiform clouds of the model essentially are of cirrus type between latitudes 35° S and 35° N. Furthermore, the build-up time during the first 48 hours is clearly seen, especially for the high clouds.

The GOES-WEST imagery shows that the area of cirrus (and underlying convection), which is missing on the predicted pictures (over the central Pacific), is a persistent feature practically throughout the whole forecasting period. On this projection it is furthermore indicated that the bridge of predicted cirrus clouds across the equator occurs about 15–20 degrees to the east of the observed cross-equatorial clouds.

Although there are some features that are not well predicted, the general resemblance between forecast and observed cloudiness is noteworthy. The model-produced areas that are free of high clouds in the tropics and subtropics agree well with the observed counterparts. The pattern of predicted cirrus, naturally agrees to the same degree, but, as mentioned earlier, an appraisal of forecast water content (and local coverage) requires a study involving dynamical considerations.

The cloud systems connected with middle and high latitude cyclone waves are worth paying attention to also in the displays of Plate 2. A longer period for verification and a view of systems in the southern hemisphere is seen, which is not shown otherwise in this report. It is easy to follow individual frontal waves across the disc in both hemispheres, or alternatively study the time variation of cloudiness at a particular point.

3.3. *Cross-sections containing clouds*

In order to get a more detailed and quantitative picture of the appearance of the model clouds a few cross-sections have been prepared. The synoptic conditions of the time period covered in the present experiment do not offer any reasonably pure "structure model" situations. Furthermore, a time-height section will be shown, which exhibits the cloud situation during the prediction period at a fixed location. Finally, an instantaneous cross-section illustrating a model stratocumulus case, mentioned in the previous subsection, will be presented.

Fig. 2 is a height–latitude cross-section along longitude 157.5° W from 40° N to 75° N of day 5. The height is calculated from sigma according to the standard atmosphere. As seen from Plate 1, a frontal system with its deep cloudiness is crossed twice. Both cloud water content (mixing ratio) and cloud cover (per cent) are displayed in Fig. 2. Since the model orography across Alaska is low, orographic effects probably are negligible, except possibly for the lowest levels. There is a cirrus shield with low water content extending northward from the system. This shield has a local coverage of about 70%. Moving southwards it is found that a more or less completely overcast region, beginning with cirrostratus, occupies some 7–8 degrees latitude. The southern portion (centred around 45° N) is somewhat narrower. In both portions, the band of pronounced cloud water density and precipitation has a width of about three degrees latitude.

Fig. 3 shows the predicted cloud situation as a function of time and height at the point 45° N, 60° W (eastern end of Nova Scotia). As seen from Plate 1, a development begins to the southeast of the point and the northeastward moving system then passes to the east of it. The picture exhibited in Fig. 3 calls to mind the classical structure model of stratiform frontal clouds; the observed cloudiness gradually changes from cirrus via cirrostratus and nimbostratus to stratus/stratocumulus. However, this interpretation requires a slight modification. The clouds existing until about 12 GMT, 19 January (day 3.5) belong to the warm front system that passes the point at some distance. The low clouds observed at that time and later rather belong to the north-northwesterly flow in the

Plate 1. Predicted stratiform cloud water mixing ratio at prediction times as indicated on the individual pictures (forecast day 1 is 00 GMT 17 January 1979). Red for low clouds (summation over the layer $1 \geqslant \sigma \geqslant 0.72$); yellow for middle clouds ($0.72 \geqslant \sigma \geqslant 0.37$); blue for high clouds ($0.37 \geqslant \sigma$). Trace value for respective category is 0.18×10^{-3}, 0.15×10^{-3} and 0.05×10^{-3}. Full lines are 85 kPa isohypses with spacing 80 gpm. Note: on day 4, full lines are the 85 kPa isotherms. Mosaics of the polar orbiting satellite (TIROS-N) IR black and white pictures cover the period 19–20 January. Note that time varies around the disc as indicated by the GMT clock at the circumference.

Plate 2. Predicted stratiform cloud water mixing ratio at day 1 through day 5. Colouring is as described for Plate 1. Isohypses of the 50 kPa surface are shown; spacing 40 gpm, but poleward of approximately 35–40° the spacing is 160 gpm. The projection is the same as for the geostationary satellite GOES-WEST (centred at 135° W), from which pictures (IR) are shown at corresponding times.

The plates have been printed at Tryckindustri AB, P.O. Box 3054, S-171 03 Solna, Sweden.

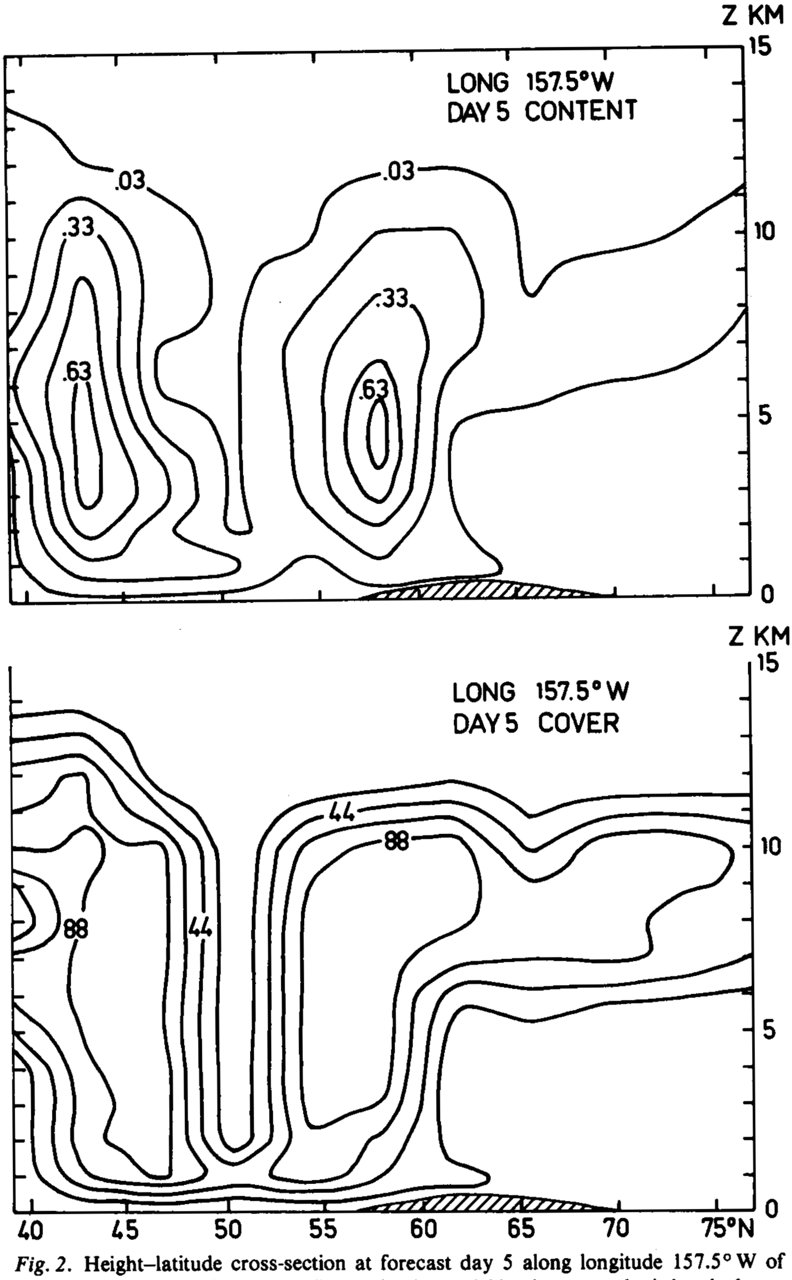

Fig. 2. Height–latitude cross-section at forecast day 5 along longitude 157.5° W of cloud water content in g kg^{-1} (top) and cloud cover in per cent (bottom). The model land topography is hatched.

rear of the low pressure. A clearing beginning at all levels is distinctly displayed on day 3.5, especially on the graph of the cloud cover. It is also interesting to note that the straticumulus coverage during the last 48 hours is approximately 50–60%.

The cloud water content shown in Figs. 2 and 3 compares well with amounts measured in real, frontal systems (see, e.g., Matveev, 1967).

As a third case in this presentation of cross-sections, we will consider the situation of day 4 over the Pacific Ocean south of Kamchatka. There is a large area of low clouds in the flow of cold air

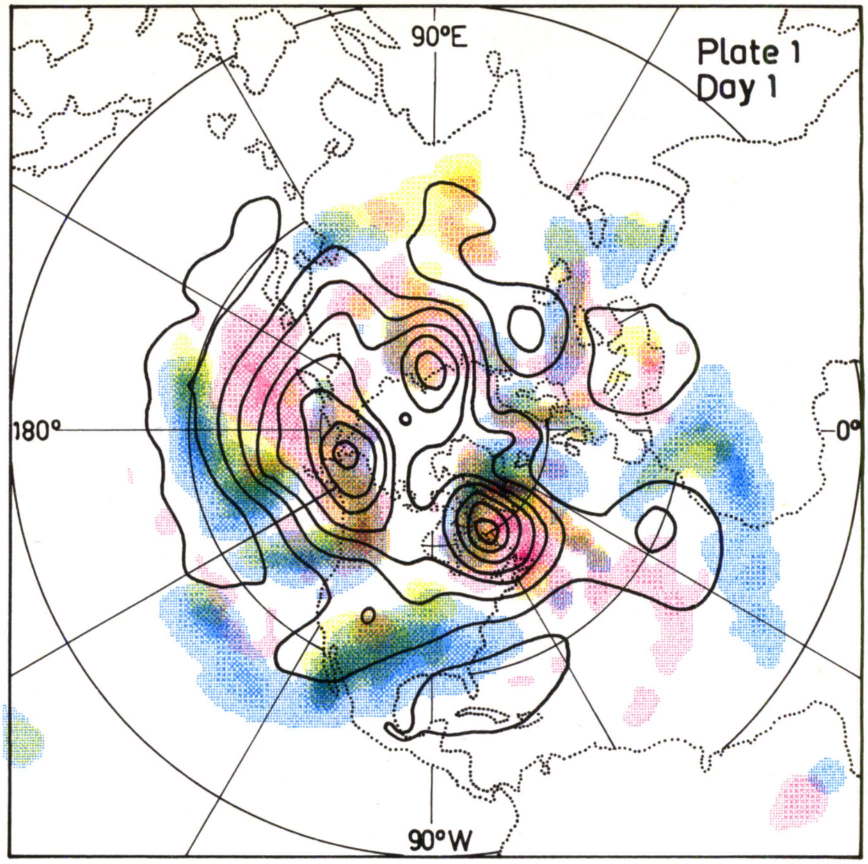
90°E
Plate 1
Day 1
180°
0°
90°W

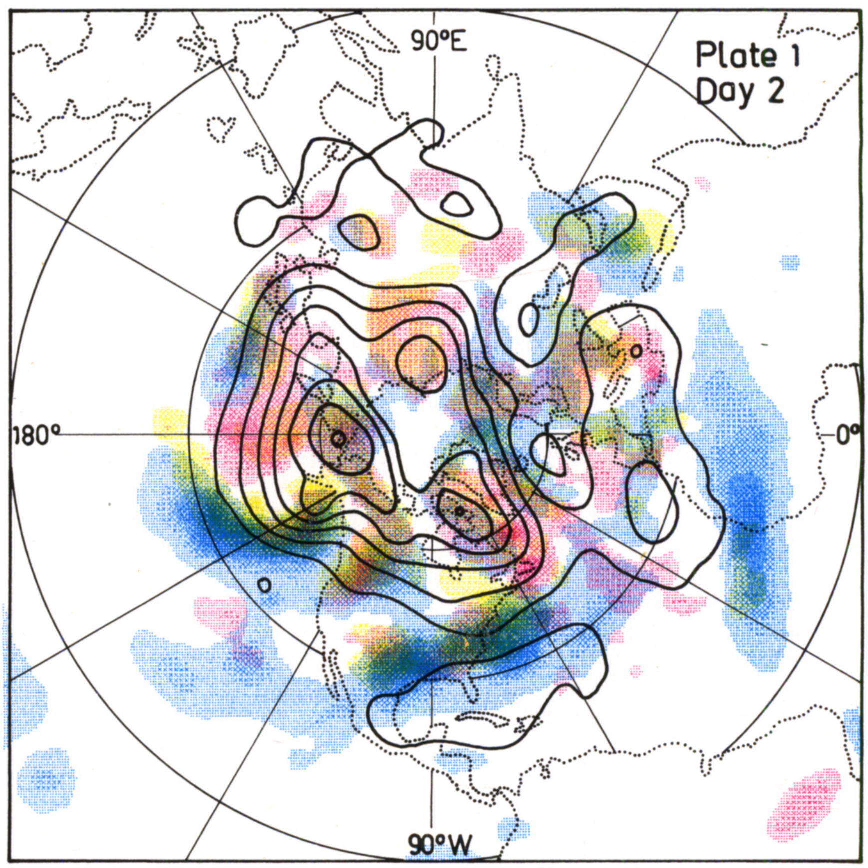
90°E
Plate 1
Day 2
180°
0°
90°W

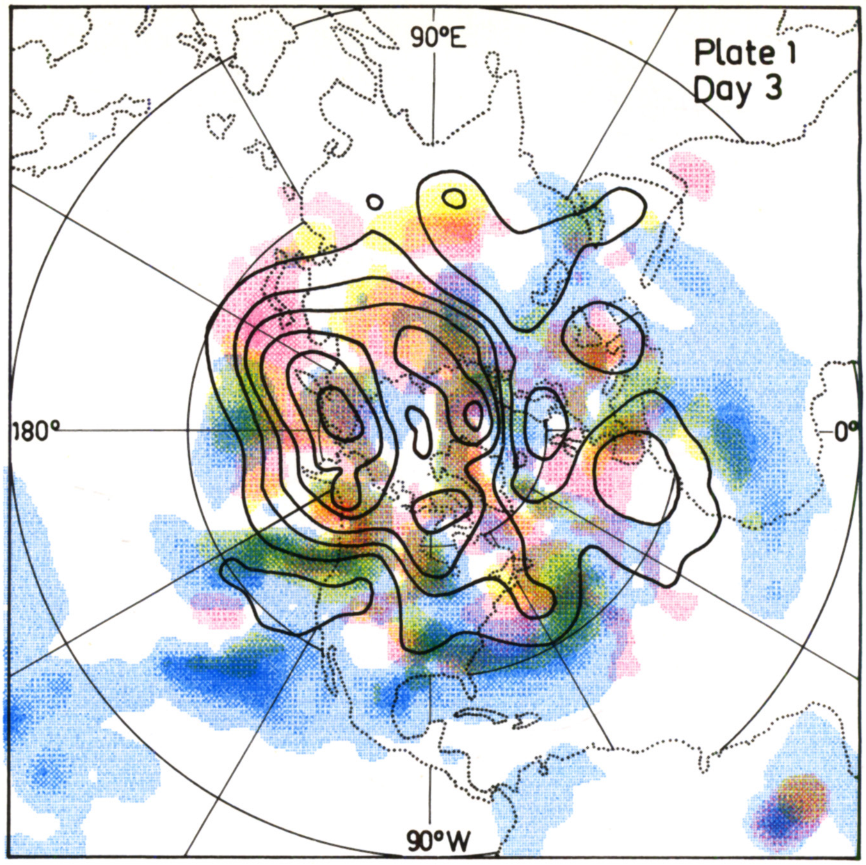
90°E
Plate 1
Day 3
180°
0°
90°W

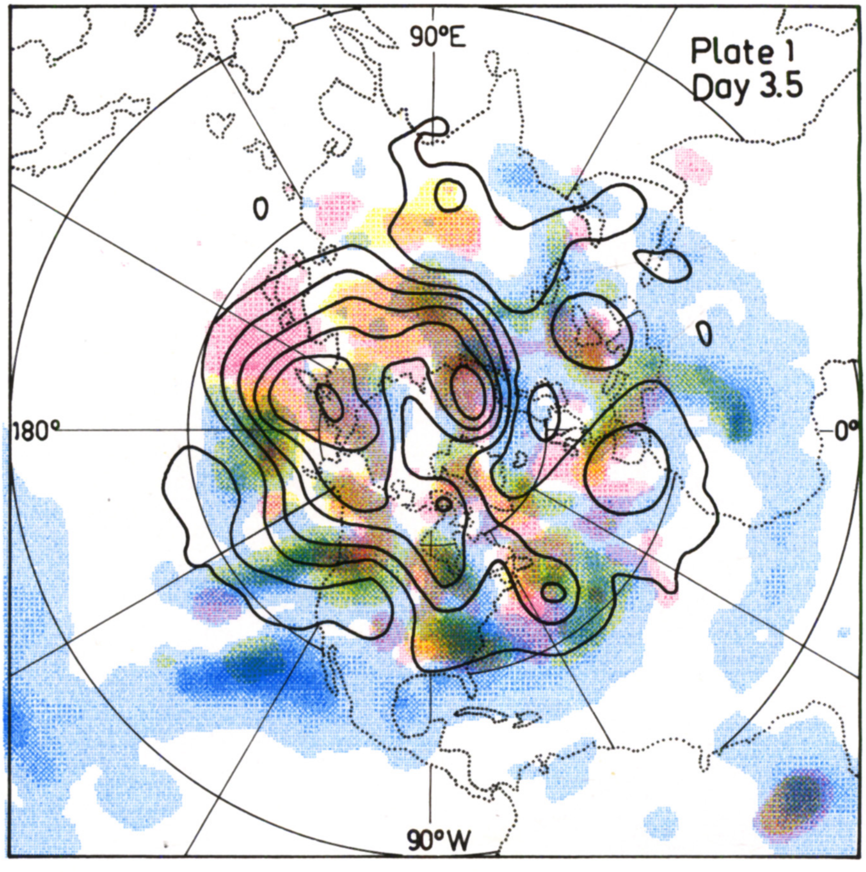
90°E
Plate 1
Day 3.5
180°
0°
90°W

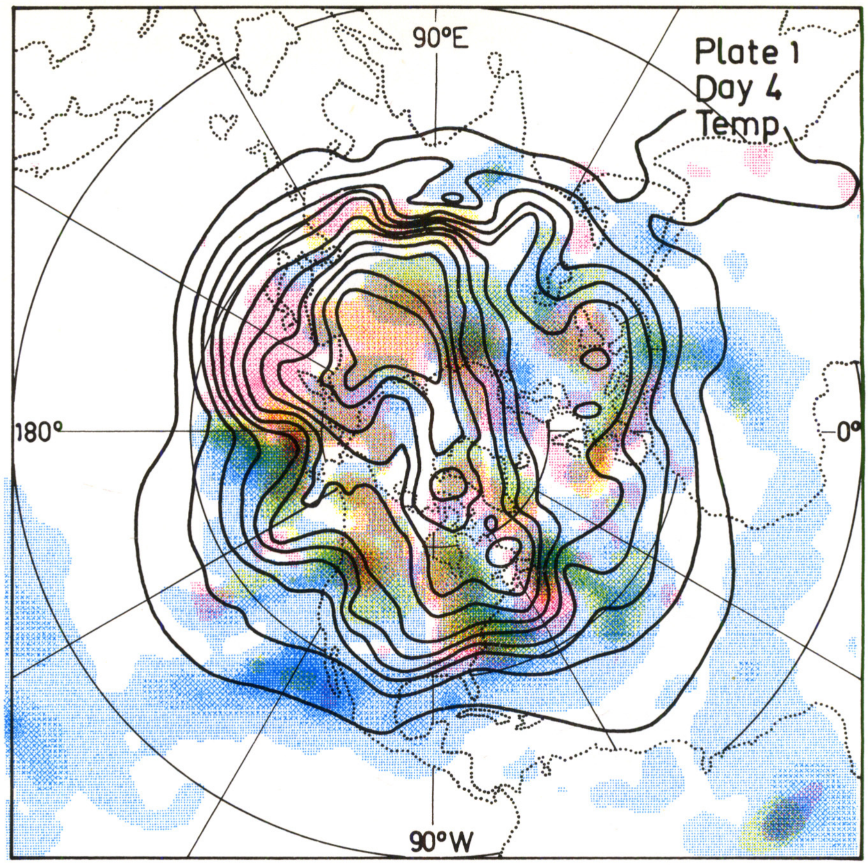
Plate 1
Day 4
Temp
90°E
180°
0°
90°W

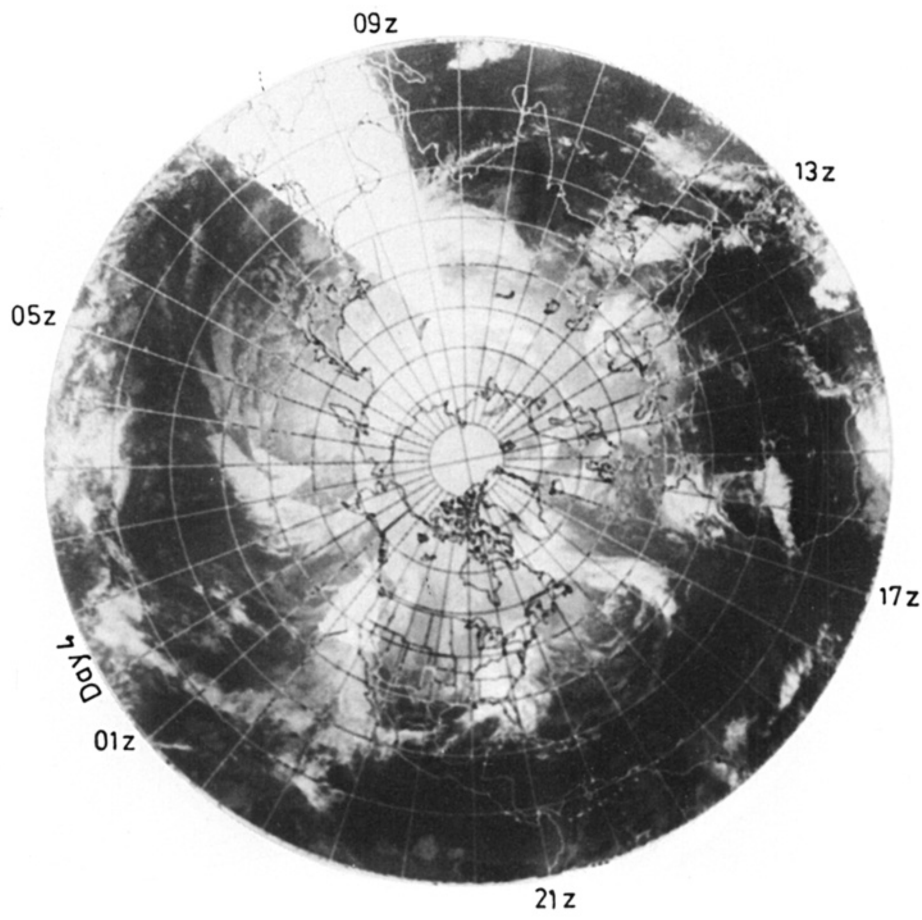
09z
13z
05z
17z
Day 1
01z
21z

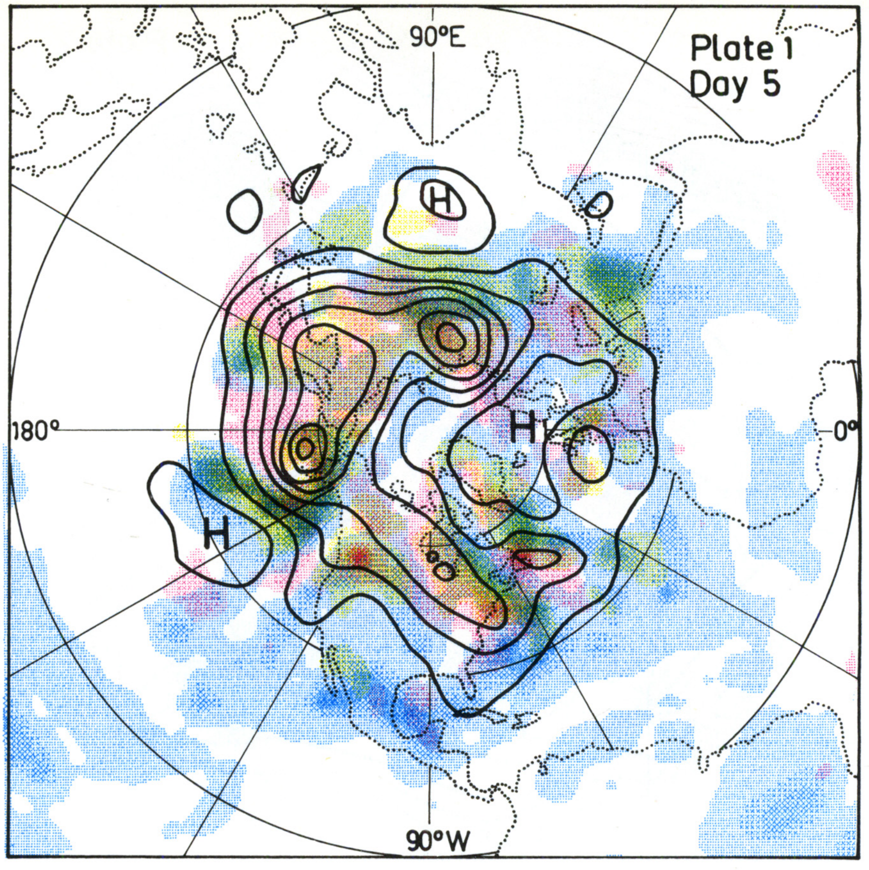
Plate 1
Day 5
90°E
180°
0°
90°W
H
H
H

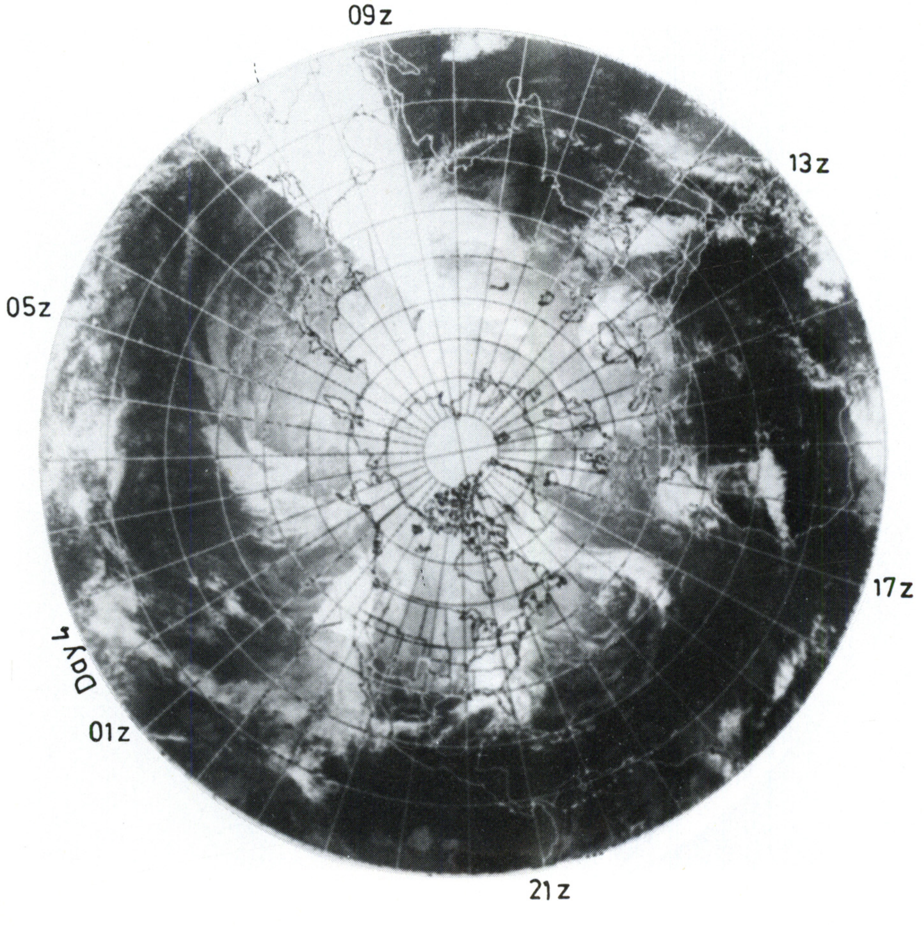
09z
13z
05z
17z
Day 6
01z
21z

Plate 2
Day 1

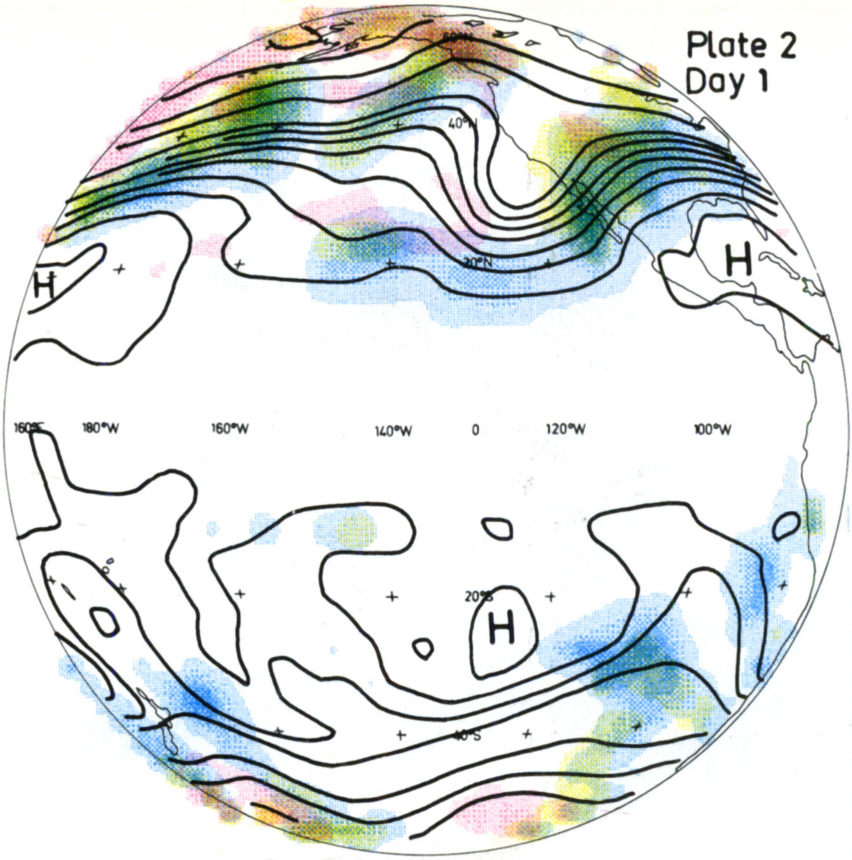

40°N
20°N
H
H
180°W
160°W
140°W
0
120°W
100°W
20°S
H
40°S

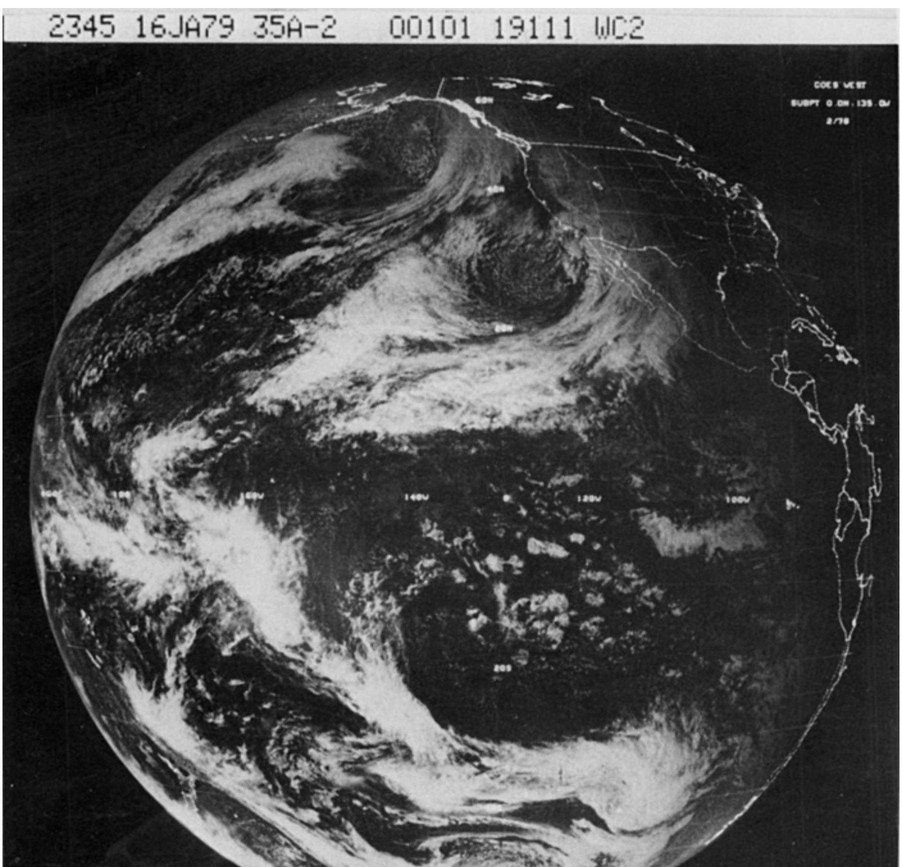

2345 16JA79 35A-2 00101 19111 WC2

Plate 2
Day 2

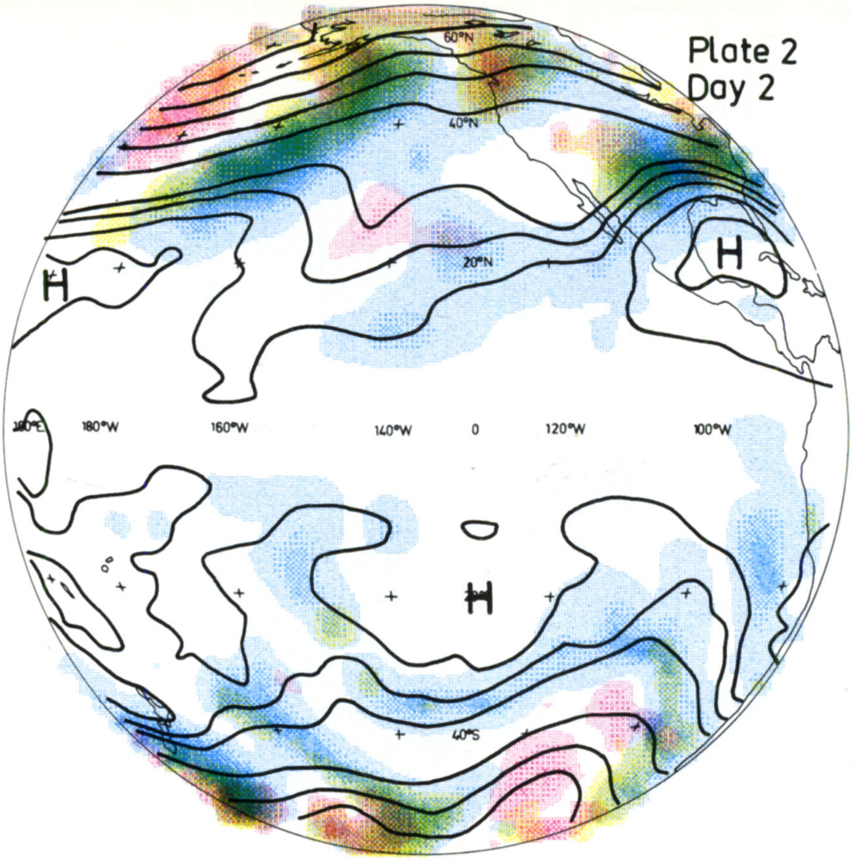

60°N
40°N
20°N
H
H
180°E
180°W
160°W
140°W
0
120°W
100°W
H
40°S

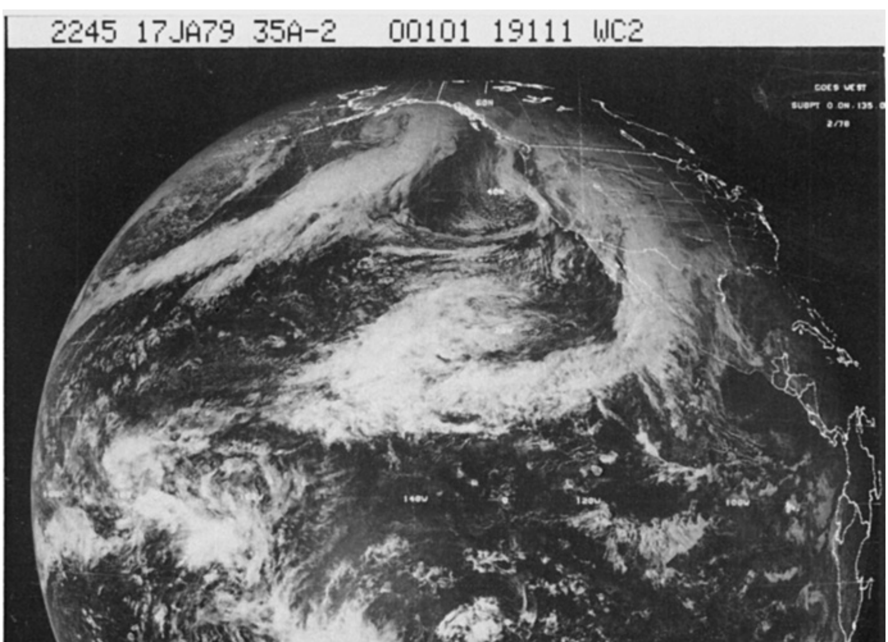

2245 17JA79 35A-2 00101 19111 WC2

Plate 2
Day 3

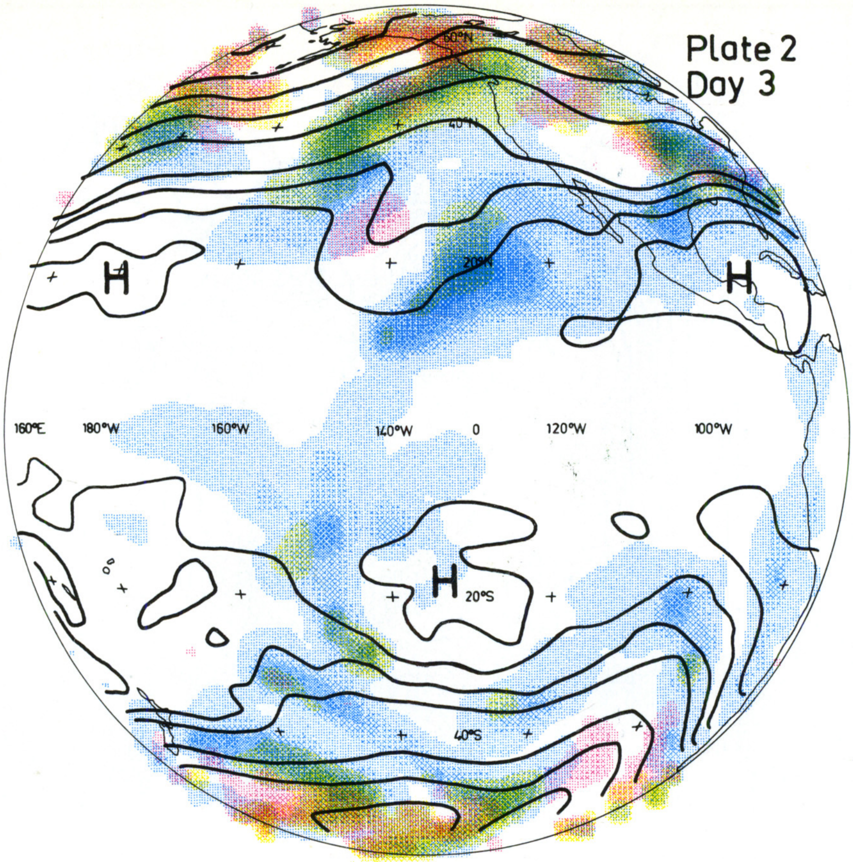
60°N
40°N
20°N
H
H
H
160°E
180°W
160°W
140°W
0
120°W
100°W
20°S
40°S

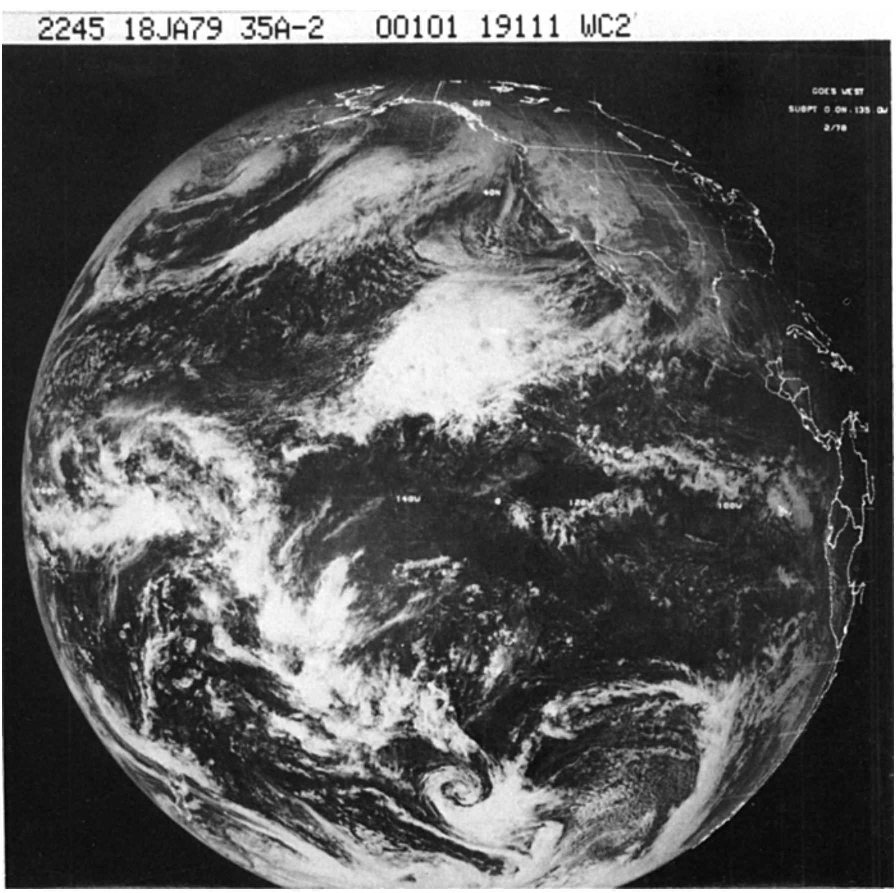
2245 18JA79 35A-2 00101 19111 WC2

Plate 2
Day 4

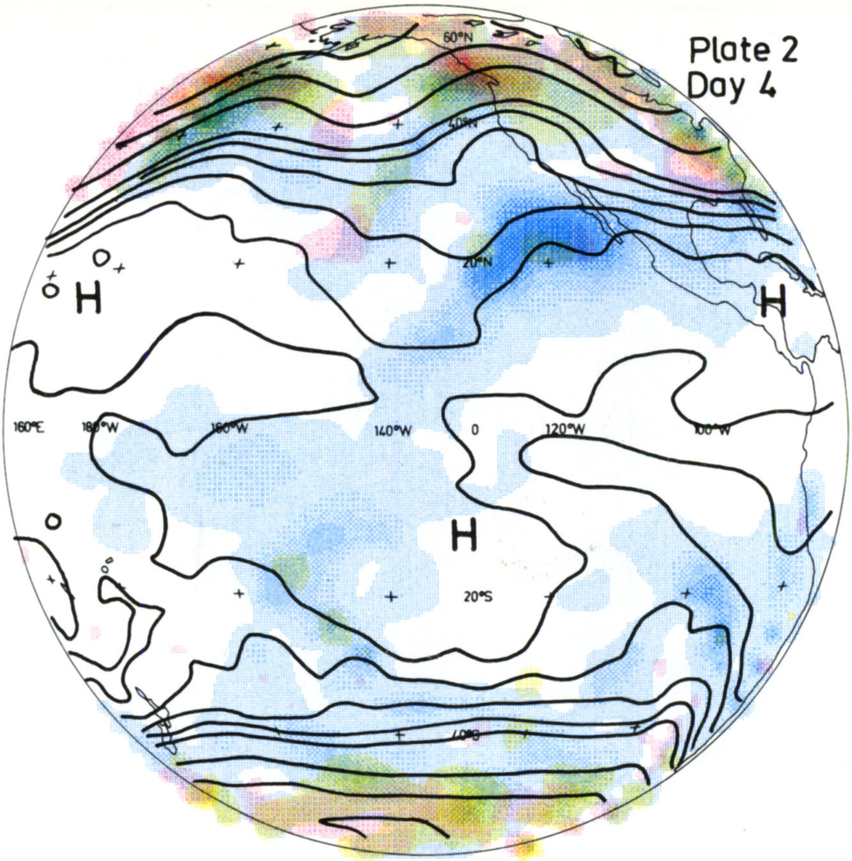
60°N
40°N
20°N
H
H
H
160°E
180°W
160°W
140°W
0
120°W
100°W
20°S


2345 19JA79 35A-2 00101 19111 WC2

Plate 2
Day 5

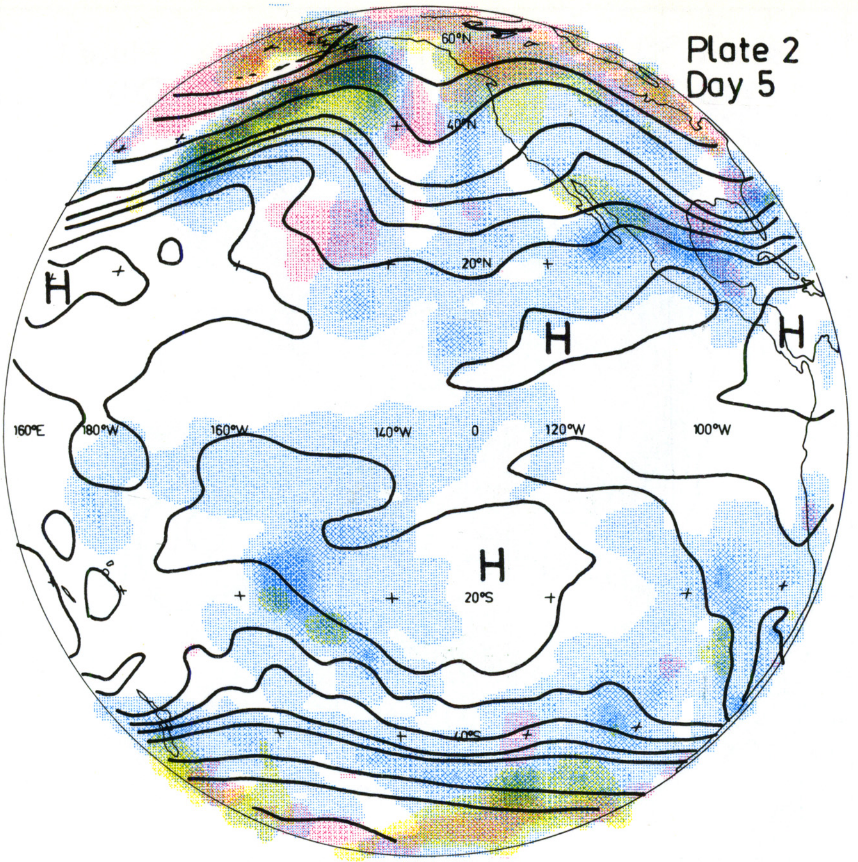
60°N
40°N
20°N
H
H
H
H
160°E
180°W
160°W
140°W
0
120°W
100°W
20°S
40°S

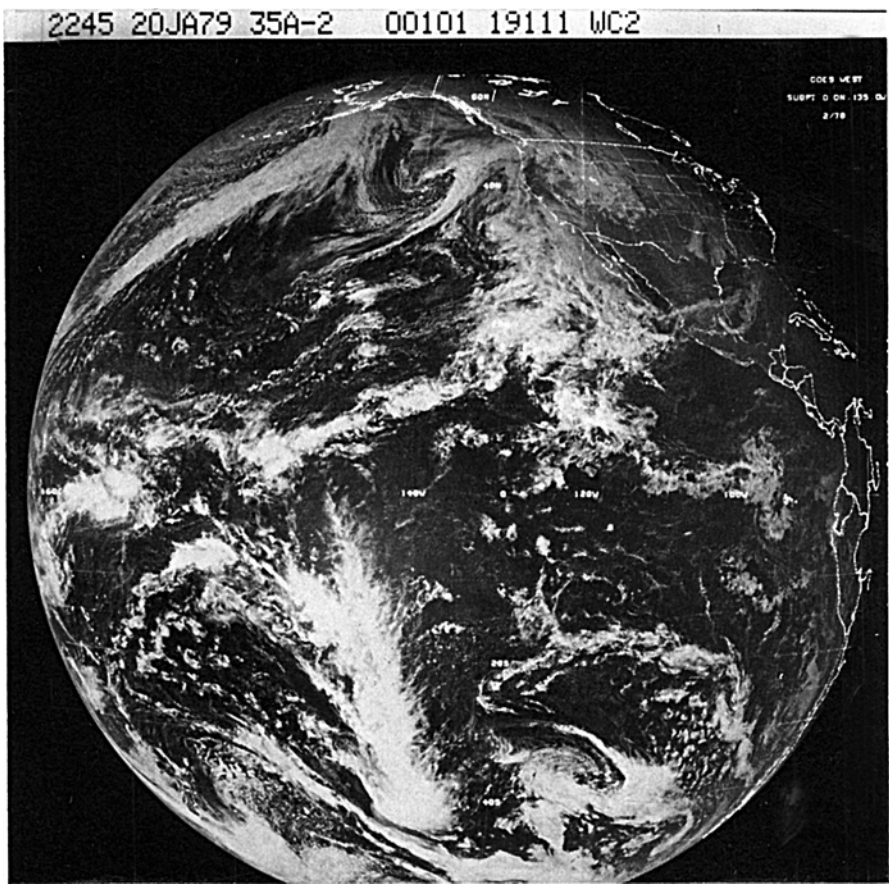
2245 20JA79 35A-2 00101 19111 WC2

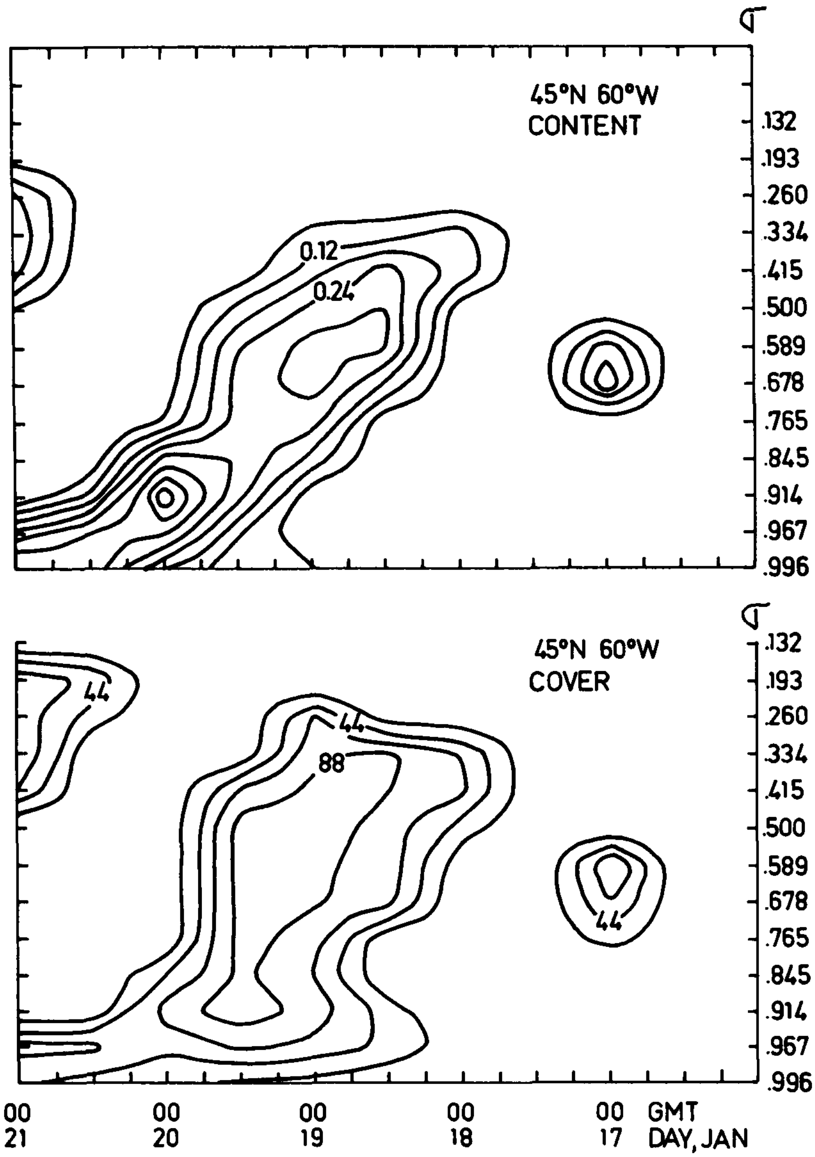

Fig. 3. Time–height diagram at 45° N, 60° W for predicted cloud water content in g kg^{-1} (top) and cloud cover in per cent (bottom). Note that time increases from right to left on the abscissa.

from northwest (see Plate 1). Fig. 4 contains a height–latitude plot of the cloud water content along longitude 161.25° E, from 25° N to 60° N. The same figure also shows the model temperature at four latitudes of the cross-section and the appropriate clouds are indicated by stippling in these profiles. The figure presents a qualitatively realistic picture of stratocumulus trapped under a temperature inversion. To the extent the thickness of that cloud deck is realistic could possibly be discussed. It deserves pointing out that no particular coupling to the unstable, turbulent boundary layer is included in the computations. Such considerations might result in a reduced thickness, in the first place probably from the top because of subgrid scale entrainment of dry air from above.

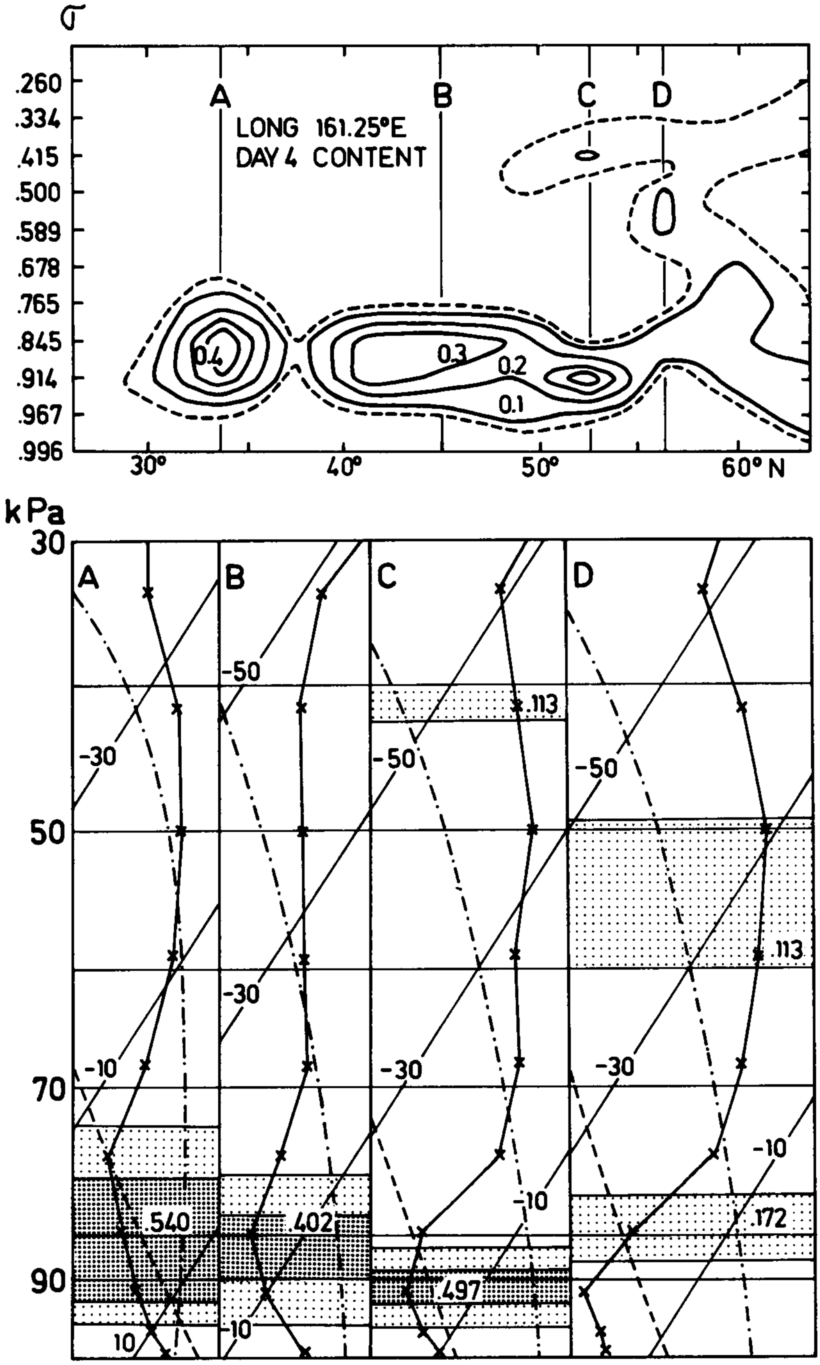

Fig. 4. Height–latitude cross-section at forecast day 4 along longitude 161.25° E of cloud water content in g kg^{-1} (top). Spacing 0.1 g kg^{-1}; dahsed line is for 0.05 g kg^{-1}. The bottom panel displays profiles of predicted temperature at latitudes indicated by vertical lines A, B, C and D in the top graph. Sigma level values are plotted assuming surface pressure 100 kPa. Cloud layer is represented by stippling; sparse for cloud water mixing ratio between 0.1×10^{-3} and 0.3×10^{-3}; denser for mixing ratios greater than 0.3×10^{-3}; maximum value is given at its appropriate level. Dry and moist adiabats are indicated by dashed and dash-dotted lines respectively.

Radiation processes, which are left out in the present study, are furthermore likely to cause a modified appearance of that deck.

In the southernmost profile (A), the cloud is remarkably deep. Convective instability exists over a deeper layer at this point than at the others farther north. In this report we merely note that the depth of that layer evidently is insufficient for application of the parameterization scheme for moist convection. Whether the condensation is treated as stratiform or convective in this layer may be of importance since the two alternatives distribute sensible heat and moisture differently in the vertical. An investigation of this matter is of importance in order to find out under which conditions one or the other alternative should be applied. Concerning what was said earlier in this paragraph, a related study could be suggested, the intention of which is to utilize recent ideas about the stratocumulus-capped mixed boundary layer (see e.g., Deardorff, 1980, where additional references on the matter may be found).

The cloud cover parameter has a representative value of 65–70% for the stratocumulus layer. The traces of middle and high clouds in the northern part of the cross-section are emanating from the frontal wave over central Bering Sea.

4. Concluding comments

In the present study of a parameterization scheme for stratiform clouds, attention has been paid exclusively to the predicted distribution of clouds. Comparisons with satellite images and ordinary weather maps exhibit a high degree of realism in the evolution and patterns. As to quantitative aspects of these clouds, it is merely possible to make the statement that predicted cloud water content seems realistic judging from the few measurements in real, stratiform clouds. For the time being, it appears necessary to resort to an indirect evaluation by analyses of dynamical effects due to their influence on radiation.

Consequently, a step in testing this parameterization is to perform (long) prediction experiments with radiation incorporated. Not until then can a tuning and more definite evaluation of parameter values be done as well as a decision on possible improvements in the approach. The latter particularly concerns stratocumulus capping the boundary layer (Subsection 3.3).

In addition to testing different values of the parameters of the present condensation model it is of interest to examine effects of more elaborate formulations for some of the parameters. In SQJ it is for example proposed that the conversion rate (c_0, Subsection 2.2) should be a function of temperature in order to yield a faster conversion from cloud droplets to raindrops (Bergeron–Findeisen process) between about 260–250 K.

A comment on computing time is worthwhile. Present prediction models contain calculations of stratiform condensation of one kind or another. The scheme presented in this experiment introduces an additional set of advection terms (eq. 2.3) as well as quantities related to parameterization of the microphysics (2.3, 2.8) and of sub-grid scale cloud cover (2.5, 2.9). Therefore employment of this approach only adds a small amount of computing time in comparison with what is usually already spent on condensation calculations. The increase in time is probably a few per cent. In this respect, the present scheme hardly introduces any problems. The fact that the scheme involves one more prognostic variable might rather be of some concern since additional storing space in a computer is required.

5. Acknowledgements

The author gratefully acknowledges the assistance of Mr Henry Larsson, Department of Meteorology, University of Stockholm, who did the programming for the implementation of the parameterization into the ECMWF model; Mr Larsson also programmed the interpretation of model cloud data for colour plotting. The author likes to thank the Research section of ECMWF for making the prediction model program available; the help from staff members of the same section on concrete programming questions is appreciated. The author is indebted to Dr Arnold Gruber, NESS, NOAA, for supplying the GOES-WEST imagery. The model integrations were run on the ECMWF computer on the time allocated for Sweden as a member country.

The study has been financially supported by the Swedish Science Research Council under contract numbers G 2923-100 and G-UR 2923-102.

REFERENCES

Burridge, D. M. and Haseler, J. 1977. A model for medium range weather forecasting—adiabatic formulation. *ECMWF Technical Report No. 4.*

Deardorff, James W. 1980. Stratocumulus-capped mixed layers derived from a three-dimensional model. *Boundary Layer Meteorology 7*, 495–527.

Hollingsworth, A., Arpe, K., Tiedtke, M., Capaldo, M., Savijärvi, H., Åkesson, O. and Woods, J. A. 1980. Comparison of medium range forecasts made with two parameterization schemes. *ECMWF Report No. 13.*

JSC, 1980. *Catalogue of numerical atmospheric models* for the First GARP Global Experiment, Part I, 287–340, ICSU/WMO, Joint Scientific Committee, Geneva, April 1980.

Marshall, J. S. and Palmer, W. McK. 1948. The distribution of raindrops with size. *J. Meteorology 5*, 165–166.

Mason, B. J. 1971. *The physics of clouds.* Oxford University Press.

Matveev, L. T. 1967. Chiefly chapter 21 in *Physics of the atmosphere.* Israel Program for Scientific Translations, Jerusalem.

Pruppacher, Hans R. and Klett, James D. 1978. *Microphysics of clouds and precipitation.* D. Reidel Publishing Company.

Sundqvist, H. 1978. A parameterization scheme for non-convective condensation including prediction of cloud water content. *Quart. J. Roy. Met. Soc. 104*, 677–690.

Sundqvist, H. 1980. Stratiform clouds as a prognostic variable in a global model: results from a five day forecast Univ. of Stockholm, Dept. of Met. *Report DM-31.*

Tiedtke, M., Geleyn, J.-F., Hollingsworth, A. and Louis, J-F. 1979. ECMWF Model-parameterization of sub-grid scale processes. *ECMWF Technical Report No. 10.*

РЕЗУЛЬТАТЫ ПЯТИДНЕВНОГО ПРОГНОЗА НЕКОНВЕКТИВНЫХ ОБЛАКОВ С ПОМОЩЬЮ ГЛОБАЛЬНОЙ МОДЕЛИ

Схема параметризации конденсационных процессов неконвективных облаков включая и водность облаков как прогностическое переменное вводится в численную модель глобального прогноза. Рассматривается поведение облаков в модели при интегрировании её на срок 5 дней. При анализе полученных результатов, облака были сгруппированы в 3 класса: низкие, средние и высокие и таким образом, стало возможным изобразить их в свете. Эти изображении облаков также могут сравниваться с космическими снимками. Кроме того некоторые детали модели водности и обачности показаны с помощью вертикального разреза. Результаты показывают определённое сходство с действительностью и предлогается что в дальнейшем будут проводиться такие экспе-рименты в которых динамические эффекты связанные с облаками будут проанализированы.